Chinese Journal of Chemistry, **2004**, *22*, 142—147 **Article**

Adsorption Study of Methane on Activated Meso-carbon Microbeads by Density Functional Theory

SHAO, Xiao-Hong*(邵晓红) HUANG, Shi-Ping(黄世萍) SHEN, Zhi-Gang(沈志刚)
CHEN, Jian-Feng(陈建峰)

College of Chemical Engineering, Beijing University of Chemical Technology, Beijing 100029, China

A combined method of density functional theory (DFT) and statistics integral equation (SIE) for the determination of the pore size distribution (PSD) is developed based on the experimental adsorption data of nitrogen on activated mesocarbon microbead (AMCMB) at 77 K. The pores of AMCMB are described as slit-shaped with PSD. Based on the PSD, methane adsorption and phase behavior are studied by the DFT method. Both nitrogen and methane molecules are modeled as Lennard-Jones spherical molecules, and the well-known Steele's 10-4-3 potential is used to represent the interaction between the fluid molecule and the solid wall. In order to test the combined method and the PSD model, the Intelligent Gravimetric Analyzer (IGA-003) was used to measure the adsorption of methane on the AMCMB. The DFT results are in good agreement with the experimental data. Based on these facts, we predict the adsorption amount of methane, which can reach 32.3 *w* at 299 K and 4 MPa. The results indicate that the AMCMBs are a good candidate for adsorptive storage of methane and natural gas. In addition, the capillary condensation and hysteresis phenomenon of methane are also observed at 74.05 K.

Keywords activated meso-carbon microbead, methane, density functional theory, adsorption amount

Introduction

Carbonaceous porous materials play an important role in many areas of modern science and technology.[1] Activated mesocarbon microbead (AMCMB) is a new type of carbonaceous materials produced by mesophase pitches,[2,3] being widely used for many years as fillers in paints, electrical and many other fields.[4,5] The studies[6,7]on AMCMB show that AMCMBs are expected to be more ordered in structure than activated carbon fiber (ACF). The ideal structure of the MCMB is illustrated in Figure 1. However, the real materials always exhibit inhomogeneity of geometry and a single pore size can not describe the structure feature of the real pore structure well. The pore size distribution (PSD) is a useful method to characterize the porous solids.[8,9] There are many researchers who use the pore size distribution method to study the gas adsorption and fluid behavior in porous materials.[10-14] Cao and Wang[10] discussed the methane and carbon tetrachloride adsorption in activated carbon using the grand canonical Monte Carlo (GCMC) method with PSD. Ravikovitch *et al.*[11] used the density functional theory (DFT) and GCMC methods for the determination of PSD of activated carbon.

Methane is the major component of natural gas. Finding a kind of suitable nanomaterials to store methane is very important in industry process. About the methane storage and its adsorption behavior in porous carbon materials have been studied extensively.[15] In this work, we use a slit-shaped pore with pore size distribution to describe its structure in AMCMB. A combined method of density functional theory and statistics integral equation (SIE) is developed based on the experimental adsorption data of nitrogen on Meso-carbon microbeads at the temperature of 77 K. Using the PSD, the adsorption and phase behaviors of methane on AMCMB are discussed. In addition, the capillary condensation and hysteresis phenomena of methane at 74.05 K are observed. Our results indicate that the temperature is an

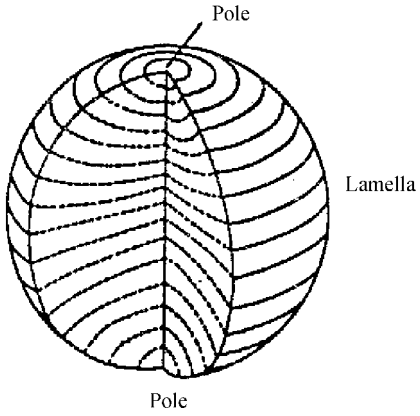

Figure 1 The ideal structure of MCMB.

* E-mail: shaoxh@mail.buct.edu.cn; Fax: +86-10-64427616
Received April 9, 2003; revised and accepted October 15, 2003.
Project supported by the Key Fundamental Research Plan (No. G2000048010) and the National Natural Science Foundation of China (Nos. 20236010, 20276004).

important factor of the hysteresis loop.

Theory and potential model

Density functional theory

Density functional theory has been proved to be a powerful method in the study of inhomogeneous fluid in confined systems.[16] In the DFT method, the density profile is obtained by minimizing the grand potential Ω. The grand potential can be expressed as:

$$\Omega[\rho(r)]=F[\rho(r)]+\int \mathrm{d}r[V(r)-\mu]\rho(r) \quad (1)$$

where $\rho(r)$, μ, $V(r)$ and $F[\rho(r)]$ are the density profile, chemical potential, external field potential and free energy, respectively. The key question in density functional theory is to calculate the free energy. In our work, the free energy is given by a first-order perturbation around the hard-sphere fluid, with the attractive part of the fluid-fluid potential interactions approximated by a mean-field term[17]:

$$F[\rho(r)]=F_{\mathrm{h}}[\rho(r)]+\frac{1}{2}\iint \mathrm{d}\boldsymbol{r}\mathrm{d}\boldsymbol{r}'\rho(\boldsymbol{r})\rho(\boldsymbol{r}')\Phi_{\mathrm{attr}}(|\boldsymbol{r}-\boldsymbol{r}'|) \quad (2)$$

where $F_{\mathrm{h}}[\rho(r)]$ is the hard-sphere part, $\Phi_{\mathrm{attr}}(|\boldsymbol{r}-\boldsymbol{r}'|)$ is the attractive part which is taken from the Weeks-Chandler-Anderson division of the LJ potential.[17] The hard-sphere part is split into an ideal part and an excess part. The excess part is adopted by Tarazona's weighted density approximation. The detailed information can be obtained from references.[18,19]

Then the equilibrium density is a solution to the following Euler-Lagrange equation:[17]

$$\mu-V=\frac{\delta F[\rho(r)]}{\delta\rho(r)} \quad (3)$$

By the solution of equation (3), the final equation of density can be expressed as[20-22]

$$\rho(r)=\exp\left\{-\frac{1}{kT}\left[f_{\mathrm{ex}}(\bar{\rho}(r))+\int \mathrm{d}r'\rho(r)f_{\mathrm{ex}}'(\bar{\rho}(r'))\frac{W(|r-r'|,\bar{\rho}(r'))}{1-\bar{\rho}_1(r')-2\bar{\rho}_2(r')\bar{\rho}(r')}+v(r)-\mu+\int \mathrm{d}r'\rho(r')\Phi_{\mathrm{attr}}(|r-r'|)\right]\right\} \quad (4)$$

where f_{ex} is the excess part of free energy, $W(|r-r'|, \bar{\rho}(r'))$ is the weighted function, $\bar{\rho}_i$ $(i=1, 2)$ is the weighted density.

Pore size distribution

In this paper, we use the statistics integral equation to calculate the pore size distribution, which is defined as the fraction of the pore volume with the width H occupying total pore volumes in the AMCMB. For a slit-shaped pore, the real adsorption amount can be written as[10,23,24]:

$$\Gamma_{\mathrm{sim}}=\sum_{H_{\min}}^{H_{\max}}\Gamma(H)g(H)\Delta H \quad (5)$$

where Γ_{sim} is the calculation result by pore size distribution, $\Gamma(H)$ is the calculated adsorption amount in a single model pore of width H, and $g(H)$ is the pore size distribution, $H_{\max}$ and $H_{\min}$ are minimum and maximum pore sizes in the cases investigated, respectively. We can obtain the pore size distribution by minimizing the deviation between the experimental isotherm and the simulation results.[24]

Potential model

Nitrogen and methane molecules are modeled as Lennard-Jones spherical molecule. The interaction between a solid wall and a fluid molecule is represented by the well-known steele's 10-4-3 potential[25,26]

$$\phi_i^{\mathrm{ext}}(z)=2\pi\rho_{\mathrm{w}}\varepsilon_{\mathrm{fw}}\sigma_{\mathrm{fw}}^2\Delta\left[0.4\left(\frac{\sigma_{\mathrm{fw}}}{z}\right)^{10}-\left(\frac{\sigma_{\mathrm{fw}}}{z}\right)^4-\left(\frac{\sigma_{\mathrm{fw}}^4}{3\Delta(0.61\Delta+z)^3}\right)\right] \quad (6)$$

where ρ_{w} is the number density of solid wall, the value of ρ_{w} is taken 114 nm^{-3},[26] the subscripts w and f represent the wall and the fluid, Δ is the distance between lattice planes, and is set to 0.335 nm, z is the normal distance between a fluid molecule and one of the solid wall. $\varepsilon_{\mathrm{fw}}$ and σ_{fw} are the cross interaction parameters, which are obtained from the Lorentz-Berthelot combing rules, $\varepsilon_{\mathrm{fw}}=(\varepsilon_{\mathrm{ff}}\varepsilon_{\mathrm{ww}})^{0.5}$; $\sigma_{\mathrm{fw}}=0.5(\sigma_{\mathrm{ff}}+\sigma_{\mathrm{ww}})$. The parameters of fluid-fluid and fluid-solid in this work are shown in Table 1.

Table 1 Parameters of fluid-fluid and fluid-solid in this work[a]

N_2		CH_4		Solid wall of AMCMB	
σ/ nm	$\varepsilon\cdot\kappa^{-1}$/ K	σ/ nm	$\varepsilon\cdot\kappa^{-1}$/ K	σ/ nm	$\varepsilon\cdot\kappa^{-1}$/ K
0.375	95.2	0.381	148.1	0.34	28.0

[a] The parameters for N_2, CH_4 and the solid wall of AMCMB are taken from Refs. 10, and 18, respectively.

Results and discussion

Nitrogen adsorption of 77 K

Nitrogen adsorption is a standard procedure for carbonaceous adsorbents.[27] The adsorption isotherm of nitrogen of 77 K is the information source about the porous structure.

The sample was prepared at the Center of Carbon

Fiber of Beijing University of Chemical and Technology. A Micromeritics ASAP 2010 apparatus was used to measure nitrogen adsorption isotherm at 77 K in the range of relative pressure P/P_0, where P_0 is the standard vapor pressure of nitrogen at 77 K. Before the measurements, the sample was out-gassed at 300 ℃ for 15 h. The BET surface area results are listed in Table 2.

Table 2 Specific surface area and average pore size measured by ASAP-2010

S_{BET}/($m^2 \cdot g^{-1}$)	*d*/nm (average)
3180	2.47

The results indicate that our sample is of high specific surface area with 3180 $m^2 \cdot g^{-1}$. The average pore size is 2.47 nm. The nitrogen isotherm at 77 K is shown in Figure 2 (the line). It can be seen that there is a large adsorption amount. Based on the experimental data, the pore size distribution was calculated in Figure 3. Obviously, the widths of pores ranging from 2.0 to 2.6 nm are the main pore size distribution of our sample. Using the density functional theory and statistics integral equation method, the nitrogen adsorption data at 77 K were calculated based on the PSD result seen in Figure 2 (the dot). it can be seen that the result from density functional theory is in good agreement with the experimental data.

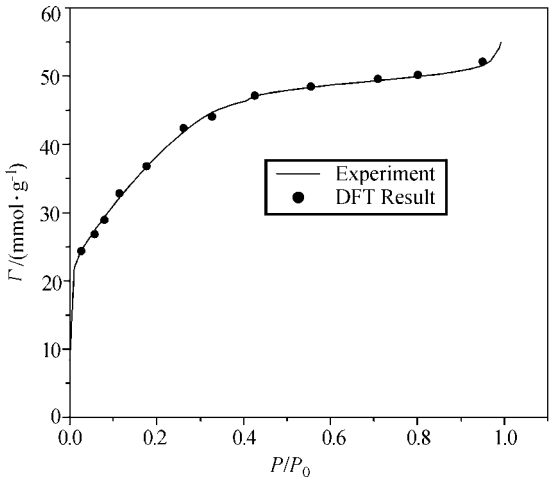

Figure 2 The comparison of experimental isotherm and DFT resluts of nitrogen at 77 K.

Methane adsorption in AMCMB

Natural gas adsorbed in nanomaterials at 4 MPa and 299 K is a promising alternative to compressed natural gas (20 MPa and 299 K) as a clean vehicular fuel and for bulk transportation.[27] In DFT calculation, we use the reduced unit to replace the adsorption density. The following equation is applied to convert the reduced unit to real unit (mmol/g)

$$\Gamma = \frac{\rho_T^*}{L\sigma_{ff}^3 \rho_c} \qquad (7)$$

$$\Gamma_{exce} = \frac{\rho_b^* - \rho_T^*}{N\sigma_{ff}^3 \rho_c}$$

where Γ is the adsorption amount, Γ_{exce} is the excess adsorption amount, ρ_T^* is the reduced density in pore, ρ_b^* is the bulk density, N is the Avogadro constant, ρ_c is the bulk density of the adsorbent, and equal to 0.4 g/cm^3 of our sample.

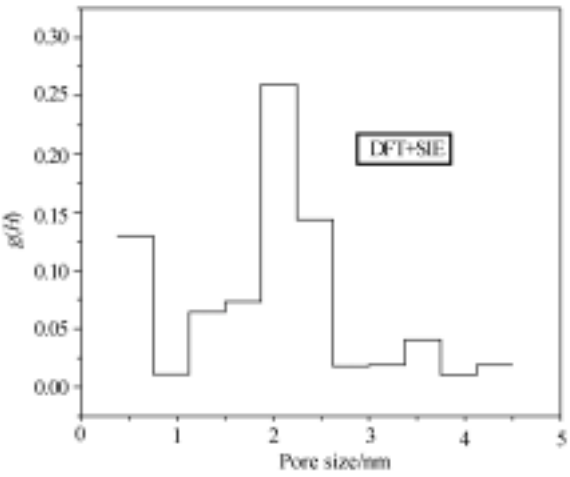

Figure 3 Pore size distribution of the sample by a combined method of DFT and SIE.

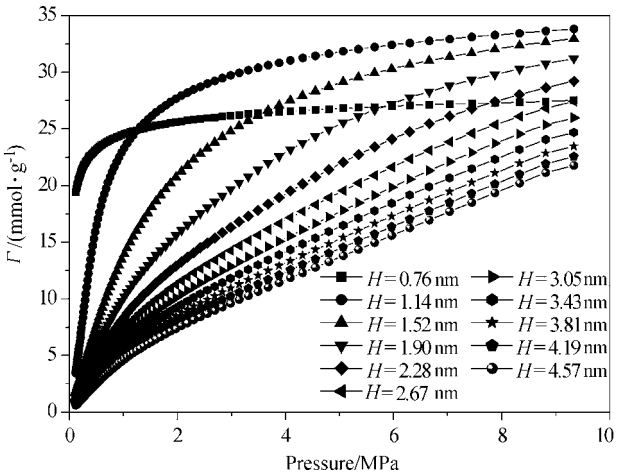

Figure 4 Adsorption of methane at the temperature of 299 K in various pores in AMCMB by DFT method.

DFT method was used to calculate the adsorption of methane at the temperature of 299 K in various pore sizes ranging from 0.76 nm to 4.57 nm of the sample, and the result is shown in Figure 4. One can see that the adsorption amount decreases with the increase of pore size on the AMCMB. The adsorption reaches saturation state quickly at the pore size of 0.76 nm because of the pore filling effect. It is noticed that AMCMB with pore

size at 1.14 nm shows the greatest uptake of adsorption because the interactions between adsorbate and adsorbent decrease slightly when the pore size increases.[10] However, there are no changes of the isotherm profiles at larger pores. Figure 5 is the excess adsorption amount in various pores of this sample. One can notice that there exists an optimal pressure to store methane for each pore size. After the optimal pressure, the excess amount decreases gradually even the pressure is increasing. When the pore size is at 0.76, 1.14, 1.52, 1.91, 2.29 and 2.67 nm, the corresponding optimal pressures are 0.88, 2.42, 4.09, 5.35, 5.96 and 6.66 MPa, respectively.

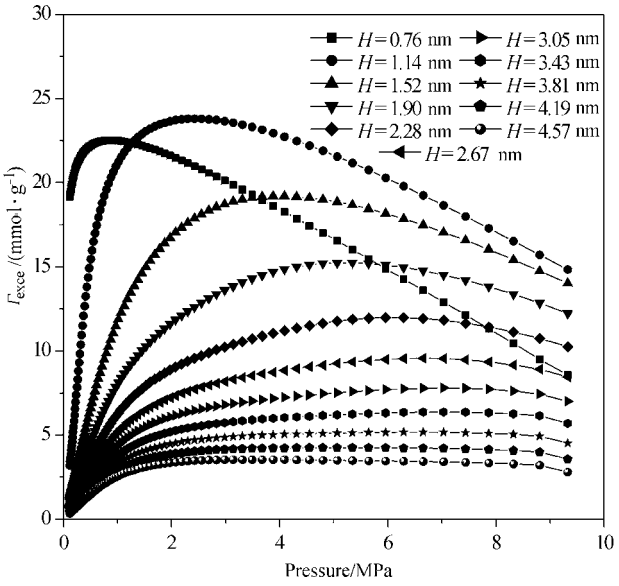

Figure 5 Excess adsorption isotherms of methane at 299 K in various pores in AMCMB by DFT method.

The combined method of DFT and SIE and the PSD model are adopted in order to get the total adsorption amount of methane on the real AMCMB. In order to verify the density functional theory and the pore size distribution method, we use an Intelligent Gravimetric Analyzer Equipment (IGA-003) to measure the adsorption of methane in the sample. Using gravimetric method to get the adsorption amount directly is the major feature of this analyzer equipment. Before the measurements, sample in the reactor was out-gassed at 300 ℃ for 15 h and the vacuum is up to 10^{-5} Pa. The pressure transducer in the gravimetric analyzer has a pressure limit at 1.0 MPa. The measurement result is shown in Figure 6 (the circle dot). The adsorption amount can reach 9.64 mmol/g at 0.97 MPa. The combined method of DFT and SIE is used to get the calculation result, which is shown in Figure 6 (the triangle pot). The comparison shows that the experimental data are in good agreement with the DFT result.

Using DFT and PSD method, we predict the adsorption amount of methane at the temperature of 299 K, as is seen in Figure 7. It can be seen that the adsorption

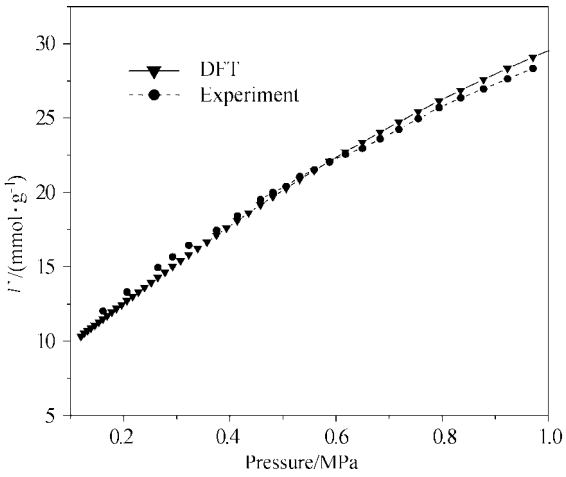

Figure 6 The comparison of DFT result by PSD and the experimental data by IGA-003.

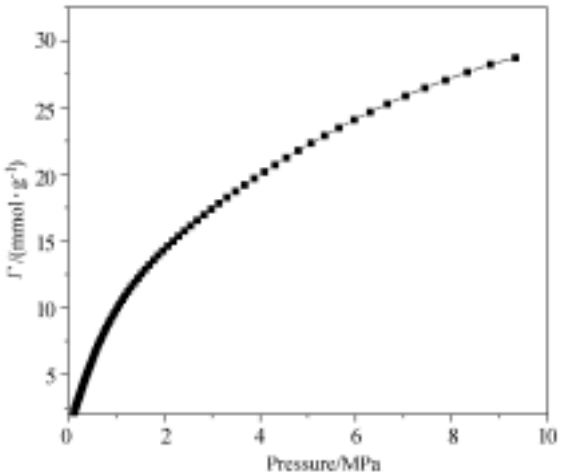

Figure 7 Methane adsorption isotherm predicted by DFT with PSD at T=299 K.

amount can reach 20.2 mmol/g (weight ratio is 32.3 *w*) at the pressure of 4 MPa. The results indicate that AMCMBs are potential material to store methane.

Methane adsorption at low temperature

Capillary condensation will occur when the temperature is below the pore critical temperature and the pore width is greater by a few times than the adsorbate molecule diameter,[28] which is usually accompanied by hysteresis phenomenon. The adsorption and desorption isotherms of methane calculated by DFT method are shown in Figure 8 and Figure 9, which show that the capillary condensation occurs at low temperature. Figure 8 is the adsorption-desorption isotherms of methane in various pore sizes. One can see that the chemical potential on the capillary condensation is increasing as the pore size is getting larger because the interaction between the adsorbate and the adsorbent is different in different pore size.[29] When the pore size is getting larger, layering transitions are observed in the adsorption isotherms. Gelb and Gubbins *et al.*[28] have discussed that

the adsorption isotherms on smooth surfaces can show stepwise behavior at relative low temperature, which is interpreted as layer-wise adsorption. The adsorbed gas prefers to complete each successive monolayer before beginning the next one. It can be concluded that the pore size is not an important factor on the hysteresis loop in comparison with the shapes in Figure 8 a—c. In order to discuss the temperature effect, the adsorption-desorption isotherms were calculated as shown in Figure 9, corresponding temperature at 74.05, 97, 117 and 157 K, indicating that the capillary condensation chemical potential (pressure) increases with temperature up. The hysteresis loop becomes narrower at the higher temperatures, and finally disappears at the hysteresis critical temperature which lies below the bulk critical temperature.[28] Based on the calculation result, it is concluded that the temperature is an important factor of the adsorption-desorption hysteresis loop.

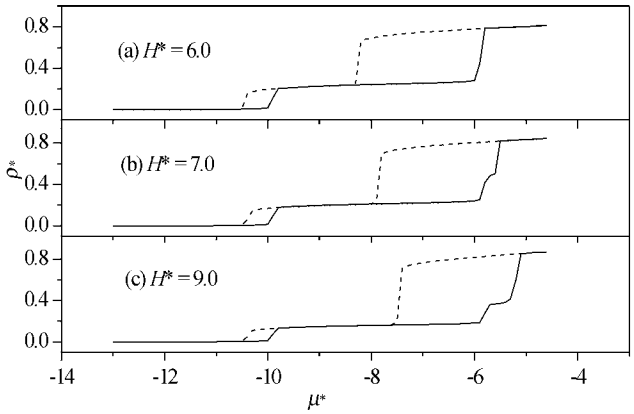

Figure 8 The hysteresis loops of methane at 74.05 K (— adsorption, --- desorption).

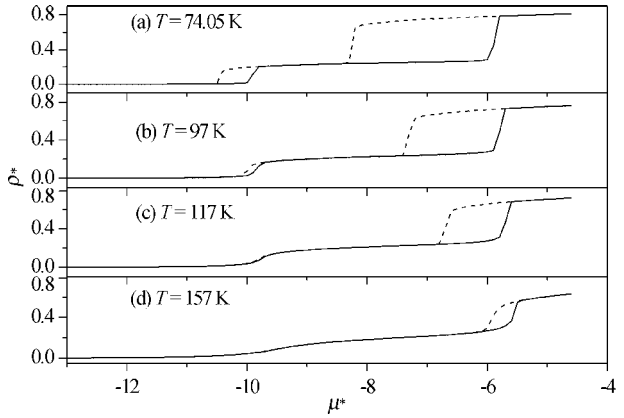

Figure 9 The hysteresis loops of methane at 2.29 nm (— adsorption, --- desorption).

Conclusions

In this paper, ASAP-2010 apparatus were used to measure the nitrogen adsorption on activated meso-carbon microbeads at 77 K. Based on the experimental data, the pore size distribution of the AMCMB was calculated by a combined method of density functional theory and statistic integral equation. The adsorption amount and the excess adsorption isotherms of methane on AMCMB with a uniform pore size ranging from 0.76 to 4.57 nm at 299 K were obtained by DFT. It is found that AMCMB with pore size of 1.14 nm show the greatest uptake of adsorption. The optimal pressures for excess adsorption amount in various pore sizes were calculated. When the pore size is ranging from 0.76, 1.14, 1.52, 1.91, 2.29 to 2.67 nm, the optimal pressures are 0.88, 2.42, 4.09, 5.35, 5.96 and 6.66 MPa, respectively.

An Intelligent Gravimetric Analyser (IGA-003) was used to measure the adsorption of methane in the AMCMB. The comparison between the experimental data and DFT result is in good agreement. We predict the adsorption of methane in high pressure at 299 K. The high adsorption amount of 20.2 mmol/g (32.3 w) was obtained at 4 MPa and 299 K. The hysteresis phenomenon of methane at 74.05 K was observed. The results indicate that the temperature is not an important factor for hysteresis loop.

Acknowledgement

The authors are grateful to Professor Wenchuan Wang for his helpful discussion and suggestions in preparation of this paper.

References

1 Simonyan, V. V.; Johnson, J. K. *J. Alloys Compd.* **2002**, *330—332*, 659.
2 Ishii, C.; Kaneko, K. *Prog. Org. Coatings* **1997**, *31*, 147.
3 Honda, H. *Carbon* **1988**, *26*, 139.
4 Esumi, K.; Kimura, Y.; Nakada, T.; Megurao, K.; Honda, H. *Carbon* **1989**, *27*, 301.
5 Shen, Z.-M.; Xue, R.-S. *Fuel Process. Techol.* **2003**, *84*, 95.
6 Ishii, C.; Matsumura, Y.; Kaneko, K. *J. Phys. Chem.* **1995**, *99*, 5743.
7 Kendall, T. T.; Gubbins, K. E. *Langmuir* **2000**, *16*, 5761.
8 Oliver, J. P. *Carbon* **1998**, *36*, 1469.
9 Lastoskie, C; Gubbins, K. E.; Quirke, N. J. *J. Phys. Chem.* **1993**, *97*, 4786.
10 Cao, D.-P.; Wang, W.-C.; Shen, Z.-G.; Chen, J.-F. *Carbon* **2002**, *40*, 2359.
11 Ravikovitch, P. I.; Vishnyakov, A.; Russo, R.; Neimark, A. V. *Langmuir* **2000**, *16*, 2311.
12 Lastoskie, C.; Gubbins, K. E.; Quirke, N. *Langmuir* **1993**, *9*, 2693.
13 Neimark, A. V.; Ravikovitch, P. I. *Langmuir* **1997**, *13*, 5148.
14 Blacher, S.; Sahouli, B.; Heinrichs, B.; Lodewyckx, P.; Pirard, R.; Pirard, J. P. *Langmuir* **2000**, *16*, 6754.
15 Zhang, X.-R.; Wang, W.-C. *Fluid Phase Equilib.* **2002**, *194—197*, 289.
16 Jiang, S.-Y.; Gubbins, K. E.; Balbuena, P. B. *J. Phys. Chem.* **1994**, *98*, 2403.
17 Weeks, J. D.; Chandler, D.; Anderson, H. C. *J. Chem. Phys.*

1971, *54*, 5237.
18 Zhang, X.-R.; Wang, W.-C. *Acta Chim. Sinica* **2002**, *60*, 1396 (in Chinese).
19 Jun, C.; Liu, H.-L.; Hu, Y. *Fluid Phase Equilib.* **2002**, *194—197*, 281.
20 Tarazona, P. *Phys. Rev. A* **1985**, *31*, 2672.
21 Tarazona, P. *Phys. Rev. A* **1985**, *32*, 3148.
22 Tarazona, P.; Marini, B. U.; Evans, R. *Mol. Phys.* **1987**, *60*, 573.
23 Heuchel, M.; Davies, G. M.; Buss, E.; Seaton, N. A. *Langmuir* **1999**, *15*, 8695.
24 El-Merraoui, M.; Aoshima, M.; Kaneko, K. *Langmuir* **2000**, *16*, 4300.
25 Steele, W. A. *Surface Science* **1973**, *36*, 317.
26 Nicholson, D. *J. Chem. Soc., Faraday Trans.* **1994**, *90*, 181.
27 Chen, X. S.; Mcenaney, B.; Mays, T.; Alcaniz-Monge, J.; Cazorla-Amoros, D.; Linares-Solano, A. *Carbon* **1997**, *35*, 1251.
28 Gelb, Lev D.; Gubbins, K. E.; Radhakrishnan, R.; Sliwinska-Bartkowiak, M. *Rep. Prog. Phys.* **1999**, *62*, 1573
29 Zhang, X.-S. *Ph.D. Dissertation,* Beijing University of Chemical and Technology, Beijing, **2001** (in Chinese).

(E0304091 ZHAO, X. J.)